Mikrochim. Acta 114/115, 213–220 (1994)

Mikrochimica Acta

© Springer-Verlag 1994
Printed in Austria

Surface and Interface Analysis of Titanium Nitride Diffusion Barriers

Marco Bonelli[1], Antonio Miotello[1,*], Lucia Calliari[2], Filippo Romanato[3], Antonio V. Drigo[3], and Alberto Carnera[3]

[1] Department of Physics, University of Trento, I-38050 Povo di Trento, Italy
[2] IRST, I-38050 Povo di Trento, Italy
[3] Department of Physics, University of Padova, Via Marzolo 8, I-35131 Padova, Italy

Abstract. Titanium nitride films were produced on silicon substrate by ion beam assisted deposition in the alternate mode: first, thin titanium layers were deposited by electron beam evaporation and then titanium nitride was formed by nitrogen implantation at room temperature; this cycle was then iterated many times in order to obtain thicker titanium nitride layers. The obtained films were characterized with respect to atomic composition by Rutherford backscattering spectrometry and nuclear reaction analysis techniques, while chemical bonding was investigated by Auger line-shape analysis. We observe that nitrogen implantation, along with the production of titanium nitride, induces silicon migration into the film. Silicon transport is connected to point defects produced by ion implantation as well as by chemical driving forces associated with silicides formation.

Key words: ion beam assisted deposition, transport processes, chemical driving forces.

Titanium nitride is an attractive material for both electronic and metallurgical applications. In fact, while having a high electrical conductivity, it behaves also as an excellent diffusion barrier in metallization processes.

TiN film deposition may be realized by means of different techniques (for instance evaporation or sputtering in reactive atmosphere) which exhibit both advantages and limitations. Ion beam assisted deposition (IBAD) plays a key role when adhesion problems are to be solved. In fact, ion implantation during the film growth succeeds in avoiding elastic energy accumulation into the film thus preserving from tensile (evaporated films) or compressive stress (sputtered films).

TiN film preparation by using IBAD with ion energy exceeding some keV may imply a considerable atomic mixing at the film/substrate interface, i.e. random transport processes of the different atomic species contribute to the interface broad-

* To whom correspondence should be addressed

ening. Moreover, when chemical affinity between the different atomic species of the substrate, film and ion beam is present, chemically guided processes may operate contributing to the final atomic composition.

By using different analytical techniques we show that repeated cycles of Ti thin film deposition on Si substrates followed by low energy N implantation allows to produce uniform and thick TiN layers. Moreover, we focused our attention to the Si transport in the interface region showing that it is related to point defects generated by irradiation as well as to chemically guided processes connected to silicides formation in the region where the N/Ti ratio is understoichiometric. Compound formation involving Si (silicides and silicon nitride) is established by analysing the Si $L_{2,3}VV$ Auger line-shape and comparing it with standards.

Experimental

The IBAD process was carried out in the alternate mode, i.e. by repeating a basic cycle, constituted by the deposition of a thin film followed by ion implantation, until the final thickness is reached. Ti atoms were evaporated with an electron gun and deposited on $\langle 100 \rangle$ Si to a thickness of 23 nm. The deposition rate was 0.1 $nm \cdot s^{-1}$. The base pressure in the chamber was about $7 \cdot 10^{-6}$ Pa. After the deposition, the sample was bombarded with 15 keV N at a fluence of $1.3 \cdot 10^{17}$ N cm^{-2}. The beam current density was kept at 5 $\mu A \cdot cm^{-2}$ and the maximum temperature reached did not exceed 320 K. Details of the IBAD apparatus and of its possible applications have been published elsewhere [1, 2].

The N range, calculated by TRIM '90, is 31 and 23 nm in Ti and TiN respectively. The chosen fluence was calculated in order to reach a N/Ti composition ratio of 1:1, in absence of Ti sputtering. (The TRIM computer code allows to calculate the primary effects induced by ions impinging on solid targets; for details see [3, 4].)

The prepared films were then characterised by using Auger electron spectroscopy (AES), Rutherford backscattering spectrometry (RBS) and nuclear reaction analysis (NRA).

Auger measurements were performed with a PHI Model 4200 Thin Film Analyzer, equipped with a Cylindrical Mirror Analyzer and a coaxial electron gun. The system base pressure was in the low 10^{-8} Pa range. Auger electrons were excited by a 3 keV, 800 nA electron beam, while target sputtering was caused by a 3 keV Ar^+ beam rastered on a 5 mm^2 area. The analyzer energy resolution was set at 0.6%.

Depth-profiles were obtained by alternating sputtering and acquisition cycles. Peak-to-peak height measurements in differential Auger spectra together with tabulated elemental sensitivity factors [5] were used to obtain concentration profiles. On the other hand, the sputtering time scale was converted into a depth scale by sputtering through a known TiN thickness.

A very high accuracy cannot be expected from this procedure of data quantification, also in view of the line-shape changes occurring in the Si $L_{2,3}VV$ and, to a much lesser extent, in the Ti $L_3M_{2,3}V$ transition. However, the atomic concentrations, derived by this procedure, are in fairly good agreement with those derived from RBS measurements.

A well-known annoyance occurring in the Auger analysis of TiN is the nearly complete overlap between the N $KL_{2,3}L_{2,3}$ and the Ti $L_3M_{2,3}M_{2,3}$ transitions. The N $KL_{2,3}L_{2,3}$ peak-to-peak intensity was obtained in the present work by subtracting the Ti $L_3M_{2,3}M_{2,3}$ contribution, as represented by a rescaled intensity of the Ti $L_3M_{2,3}V$ transition which does not interfere with other Auger transitions, through the following expression:

$$I_{N(KL_{2,3}L_{2,3})} = I_{N(KL_{2,3}L_{2,3})+Ti(L_3M_{2,3}M_{2,3})} - I_{Ti(L_3M_{2,3}V)} \frac{S_{Ti(L_3M_{2,3}M_{2,3})}}{S_{Ti(L_3M_{2,3}V)}},$$

where I and S are respectively the peak-to-peak intensity and the sensitivity factor of the specified transitions.

Depth-profiles were also used to measure the total amount of Si in the films, calculating the area under the Si profiles from the interface to the surface.

RBS and NRA were performed at Laboratori Nazionali di Legnaro by using ion beams delivered by the AN 2000 accelerator.

As for RBS a 2.0 MeV $^4He^+$ beam was used with the detector kept at the fixed scattering angle $\theta_s = 170°$. In order to improve the depth resolution of the technique the incidence angle with respect to the surface normal (θ_{in}) was varied from 0° to a maximum value of 80° for the thinnest sample. The Ti depth resolution varies accordingly from 17 to 4.3 nm. The RBS experiments were calibrated against a Ta/Si standard sample with an accuracy better than 2% [6].

The integral amount of ^{14}N in the samples was determined from NRA by using the $^4N(d, p)^{15}N$ nuclear reaction at 610 keV deuteron energy and 150° detection angle [7]. The measurements were calibrated against a Si_3N_4 standard sample whose composition is known within 5%.

Results

Concentration depth-profiles for a sample, taken as representative of the typical situations observed among the IBAD produced TiN coatings are shown in Fig. 1. Figure 1 refers to a sample produced by 4 deposition and implantation cycles (4 layers). The TiN film results quite clean, with contaminants, O and C, essentially located near the surface. Moreover, apart from the region extending below the surface up to about 20 nm, the N and Ti concentrations, as a function of depth, are essentially constant.

While the implantation dose was chosen in order to have a N to Ti composition ratio of 1 : 1, AES results indicate that the average N to Ti composition ratio is about 1.47, i.e. overstoichiometric. This fact is due primarily to the sputtering of Ti during the implantation steps. The uniform composition inside the film indicate the formation of the phase TiN; in fact, for TiN films, N/Ti composition ratios till 1.67 are reported in literature [8].

On the contrary, the region below the surface up to a depth of 20 nm is characterized by a marked N depletion and a corresponding increase in the Ti

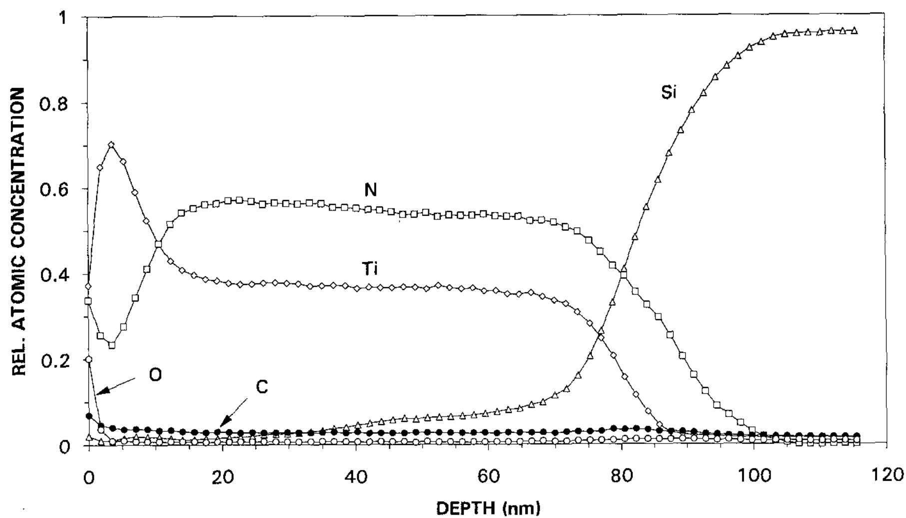

Fig. 1. AES concentration profiles for the IBAD sample produced with 4 deposition and implantation cycles (4 layers)

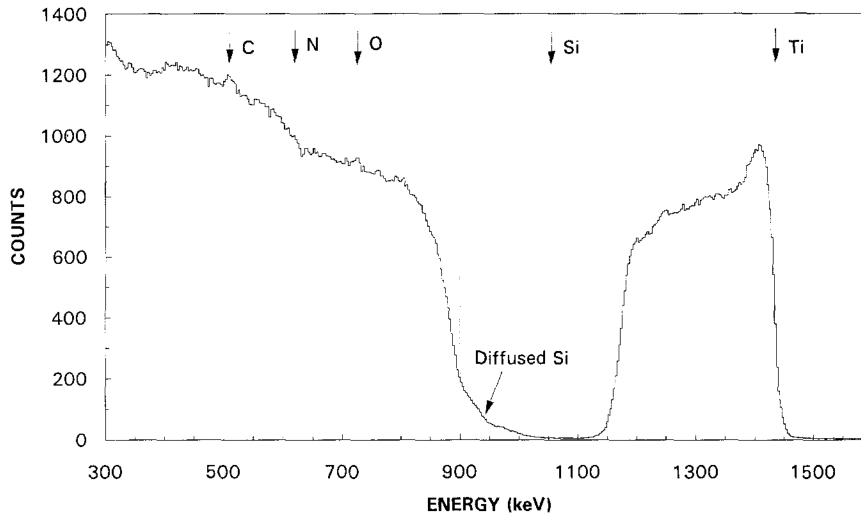

Fig. 2. RBS spectrum for the IBAD sample produced with 5 deposition and implantation cycles (5 layers). The arrows indicate the surface scattering energy from the different elements. The dashed line shows diffused Si in the film

atomic concentration. This is due to the fact that the mean projected range of the implanted N-ions in the Ti-N film amounts to a value between 23 nm (TiN) and 31 nm (Ti).

The AES results are confirmed by RBS. Figure 2 shows a 2.0 MeV He RBS spectrum of a 5 layers sample. In this case $\theta_{in} = 70°$. From the shape of the Ti signal it clearly appears that the N concentration profile slightly decreases from the interface to the surface where a N depleted zone is evidenced by the Ti sub-surface peak. This fact is inherently due to the production process as aforesaid. NRA and RBS confirm also that the average N to Ti composition ratio is about 1.48 (to compare with 1.47 of AES) and that the contaminants C and O are primarily located in the surface region.

Moreover, AES and RBS (Figs. 1 and 2) indicate a Si penetration tail into the TiN film. A systematic examination of all the samples by AES and RBS has shown that there exists an essential difference in the Si profiles between samples produced with 1–3 deposition and implantation cycles and samples with more than 3. In fact, if the coating is produced by a number of deposition and implantation cycles which is not greater than 3, not only silicon migrates through the whole overlayer, but it also gives rise to a bell-shaped peak in the sub-surface region as shown from the AES concentration profiles in Fig. 3, for the sample with 3 layers, and from the RBS spectrum in Fig. 4 (in this case $\theta_{in} = 80°$), for the sample with 2 layers. This does not occur with thicker films, since the Si concentration gradually approaches to the zero level going from the substrate towards the film surface (Figs. 1 and 2). The presence of a sub-surface Si peak was also detected by SIMS analysis.

The question now is to understand the nature of the driving forces which cause Si migration and, in the cases where the TiN coating is not too thick, the formation of a Si peak in the sub-surface region. In fact, it must be noted that the growth of such a Si peak requires the silicon atoms to move against a concentration gradient: this means that the gradient of the chemical potential is opposite to the concentra-

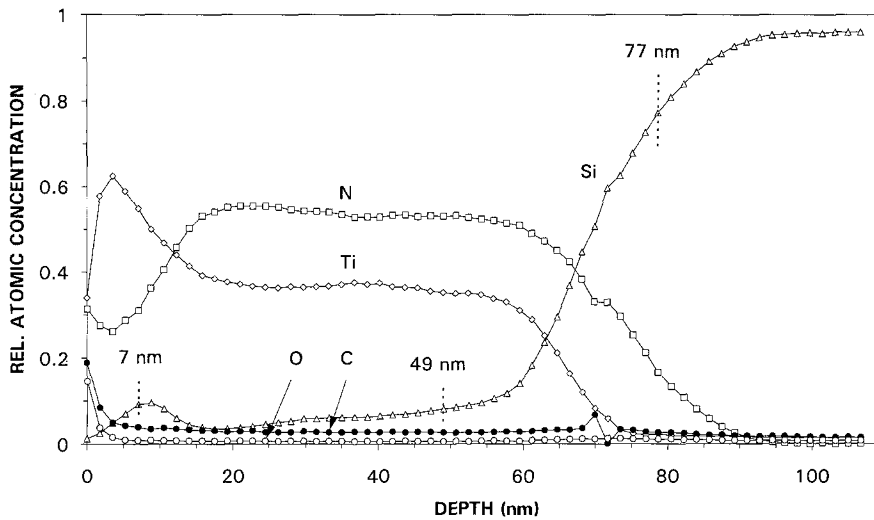

Fig. 3. AES concentration profiles for the IBAD sample produced with 3 deposition and implantation cycles (3 layers). The vertical dashed lines represent the depths where Auger line-shape analysis was performed

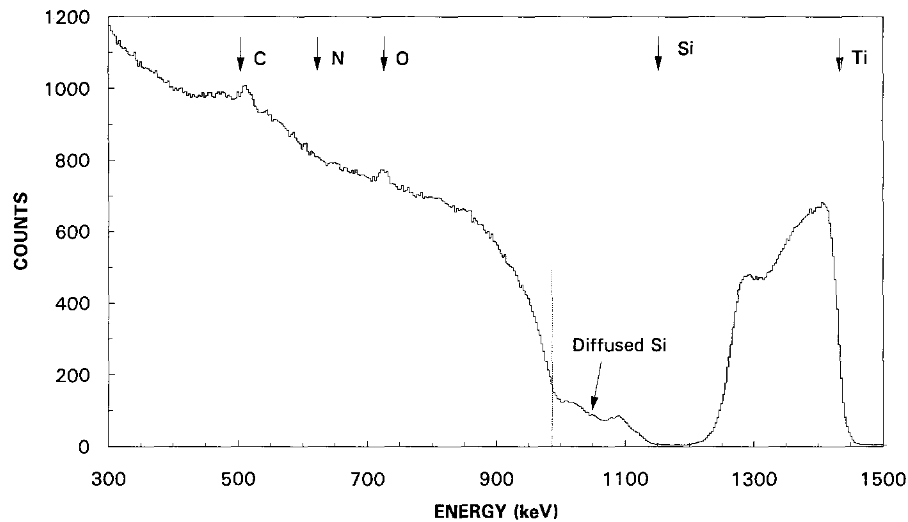

Fig. 4. RBS spectrum for the IBAD sample produced with 2 deposition and implantation cycles (2 layers). The arrows indicate the surface scattering energy from the different elements. The dashed line shows diffused Si in the film

tion gradient. However we here recall that the driving force for diffusion is a chemical potential gradient which contains concentration and activity coefficient, but also the standard chemical potential, thus the nature of the phase being considered.

To search for a possible chemical driving force in this respect, line-shape analysis was carried out on the Si $L_{2,3}VV$ Auger transition. Three significant points along the depth-profile of Fig. 3 were considered to this end and are marked by vertical dashed lines on the figure. The Si $L_{2,3}VV$ spectrum corresponding to each point is presented in Fig. 5. Integral spectra were considered. A background given by the

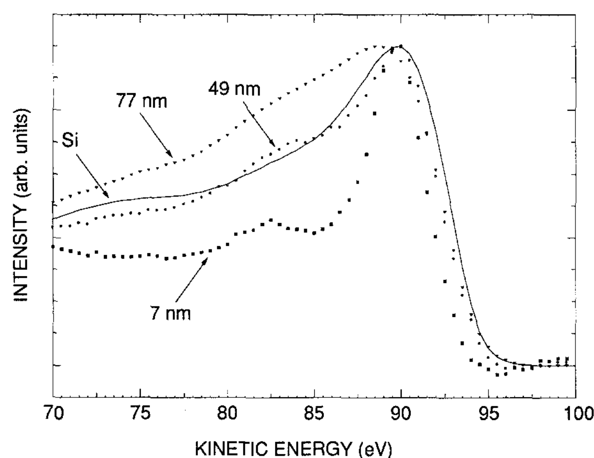

Fig. 5. Si $L_{2,3}VV$ integral Auger spectra for the sample with 3 layers at different depths (see also Fig. 3)

straight line interpolating the region to the right of the peak was first subtracted and the four spectra were then normalized to a common peak height. The depths to which they refer are marked on the figure. It can be seen that the change in the chemical environment of silicon atoms is clearly reflected in changes in the Si $L_{2,3}VV$ spectrum.

On going from the spectrum of bulk Si to that acquired at a depth of 7 nm, the main peak (associated with Auger transitions leaving 2 p-holes in the final state) does not shift in energy, while a marked decrease is observed in its width. Strictly related to this, a much better resolution of the sp shoulder (due to transitions leaving one s and one p hole in the final state) is also observed. Though to a much lesser extent, the same kind of spectral changes with respect to bulk silicon are also observed at a depth of 49 nm (and in general inside the film). On the other hand, a different situation prevails when considering the Si $L_{2,3}VV$ spectrum at a depth of 77 nm (interface region). In this case, the position of the main peak shifts to a lower kinetic energy with respect to its position in bulk silicon. Spectral weight is subtracted in this way from the high energy end of the spectrum and is added to the left of the main peak.

Keeping in mind the elemental composition in the four points along the depth-profile associated with the spectra of Fig. 5, the following interpretation of the observed spectral changes can be put forward. At a depth of 77 nm, the Ti intensity is zero, whereas a tail of implanted N is still present. The shift of spectral weight to lower kinetic energies seen here is therefore due to the Si-N interaction. A spectral trend of this kind is indeed typically observed in the Si $L_{2,3}VV$ transition whenever silicon is ionically bonded to a more electronegative species. On the other hand, the spectral changes observed at 7 nm and 49 nm are qualitatively very similar and differ only in their extent. A comparison with a Si $L_{2,3}VV$ line-shape study of the Ti/Si interface formation [9, 10] shows that these changes are related to the interaction of Si with Ti, the degree of deviation from the bulk silicon spectrum being higher the higher the Ti/Si ratio. This is indeed consistent with the excess of Ti found in the near surface region.

A mechanism of silicon out-diffusion, driven by the Si-Ti affinity, would therefore be suggested in the present case. This also explains the formation of the silicon peak

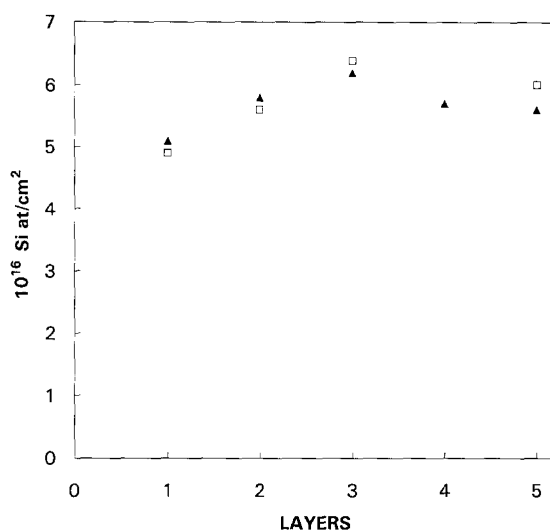

Fig 6. Total Si content in the film as a function of deposition and implantation cycles number (layer number), as detected by AES (▲) and RBS (□) techniques

in the sub-surface region of the thinner coatings, because the excess of Ti atoms in that region would represent a sort of sink for the Si atoms.

Finally, a study on the amount of Si diffused in the film as function of the deposition and implantation cycle number (layers number) was made and the results are shown in Fig. 6: both AES and RBS have detected that the Si diffusion from the substrate into the film takes place mainly during the first cycle. In the successive cycles, there occurs primarily a redistribution of Si atoms, already present in the film, with consequent progressive reduction of the Si concentration.

Conclusions

In this paper we have shown that:

a) TiN preparation with IBAD in the alternated mode results in nearly uniform and overstoichiometric TiN films with a N/Ti ratio about 1.5 for a "target" ratio of 1. However, by changing the IBAD process parameters it is possible to prepare both understoichiometric and stoichiometric titanium nitride films. On these features, we will report in a subsequent paper.

b) TiN preparation on a Si substrate employing the IBAD technique implies a relevant atomic mixing process at the Si/film interface with the Si dynamics controlled also by chemically guided processes due to silicide and Si nitride formation. To understand the occurrence of chemical processes for the Si atoms, the Si Auger line-shape was analysed and compared with Si line-shapes in silicon nitride and silicides. When both Si and N may interact with Ti then the TiN formation is favoured against silicides formation.

Acknowledgements. V. Micheli is gratefully acknowledged for the AES data acquisition.

References

[1] M. Bonelli, L. Calliari, M. Elena, M. A. Ghabashy, L. A. Guzman, A. Miotello, P. M. Ossi, *Surface Coating Technol.* **1991**, *49*, 150.

[2] M. Bonelli, L. Calliari, M. Elena, L. A. Guzman, A. Miotello, P. M. Ossi, *Vacuum* **1992**, *43*, 459.
[3] J. P. Biersack, L. G. Haggmark, *Nucl. Instr. Meth.* **1980**, *174*, 257.
[4] J. F. Ziegler, J. P. Biersack, U. Littmark, in: *The Stopping and Range of Ions in Solids* (J. F. Ziegler, ed.), Pergamon, New York, 1985.
[5] Eds.: L. E. Davis, N. C. MacDonald, P. W. Palmberg, G. E. Riach, R. E. Weber, *Handbook of Auger Electron Spectroscopy, 2nd Ed.*, Physical Electronics Division Perkin-Elmer, Eden Prairie, 1978, p. 13.
[6] C. Cohen, J. A. Davies, A. V. Drigo, T. E. Jackman, *Nucl. Instr. Meth.* **1983**, *218*, 147.
[7] M. Berti, A. V. Drigo, *Nucl. Instr. Meth.* **1982**, *201*, 473.
[8] J.-E. Sundgren, *Thin Solid Films* **1985**, *128*, 21.
[9] X. Wallart, J. P. Nys, G. Dalmai, I. Lefebvre, M. Lannoo, *Europhys. Lett.* **1989**, *10*, 587.
[10] X. Wallart, J. P. Nys, H. S. Zeng, G. Dalmai, I. Lefebvre, M. Lannoo, *Phys. Rev.* **1990**, *B 41*, 3087.